JOURNAL OF MATERIALS SCIENCE 27 (1992) 1947–1959

Effect of TiN addition on sintering behaviour and mechanical properties of WC–10Co hard metals containing Mo_2C and Ni

S. K. BHAUMIK, G. S. UPADHYAYA, M. L. VAIDYA
Department of Metallurgical Engineering, Indian Institute of Technology, Kanpur 208016, India

The aim of the present work was to substitute a portion of WC in WC–10 wt% Co hard metal by TiN by modification of the binder phase, and to produce an equivalent grade of hard metal. Sintering studies were carried out in both H_2 and H_2–N_2 (50:50) mixture. Introduction of TiN into WC–10Co hard metal resulted in a high sintered porosity, and as a consequence the mechanical properties deteriorated. Partial substitution of cobalt in WC–8.7TiN–12Co by nickel further increased the sintered porosity and led to a non-uniform microstructure. Incorporation of Mo_2C along with cobalt–nickel binder promoted a fine-grained structure, which resulted in better sintered properties than those of WC–8.7TiN–6Co–6Ni hard metal. However, hot isostatic pressing (HIP) treatment of the liquid-phase sintered alloys was effective in eliminating the large pores and thus greatly enhanced the mechanical properties. HIPed hard metal of WC–8.7TiN–12Co composition showed properties almost equivalent to those of WC–10Co hard metal.

1. Introduction

Developments in the field of hard metals are mainly related to raw materials supply, economic factors and the general object of saving energy and strategically important materials, apart from enhancing the performance of the existing grades. Many attempts have been made in the past to design new systems which can be compatible with WC-based hard metals. Very little success has been achieved in this regard, and WC-based hard metals remain by far the major competent materials in the field of cutting and wear-resistant applications. However, some success has been achieved in substituting a portion of WC to produce an equivalent grade. One such example is WC–TiN–Co hard metal which has a higher hardness and a lower transverse rupture strength than those of WC–Co cemented carbide [1]. Any such replacement of heavy expensive transition metal by cheaper, abundant and specifically light metals is of great interest at present.

Cobalt is the most traditional binder metal used for WC-based hard metals, but due to its high cost and limited resources, efforts have been made to replace cobalt by other iron-group metals. It is reported in the literature [2, 3] that the same or even superior sintered properties to those of WC–Co hard metals can be achieved through using a Co–Ni binder instead of straight cobalt. On the other hand, as far as the wettability is concerned nickel is believed to be a better binder metal for titanium carbide/nitride [4]. The wettability is further improved when molybdenum is also present in the binder phase along with nickel [5].

The aim of the present work was to partially substitute WC in WC–10Co hard metal by TiN by modification of the binder phase, so as to produce an equivalent or a better grade of alloy. A lower cost is expected due to the lower density of such hard metal. Furthermore, nitrogen-containing hard metals have been reported to have increased strength and oxidation resistance compared with those of WC–TiC–Co hard metals [1, 6].

2. Experimental procedure

The characteristics of different powders used in this study are given in Table I. The starting composition of the hard metal, i.e. WC–10Co, corresponded to approximately 16.5 vol% binder phase. All the subsequent compositions developed later were tailored so that the volume fractions of hard phase and binder remained constant and equal to those in the initial WC–10Co hard metal. The respective mass percentage additives in various hard metal compositions are given in Table II.

The premix of carbides, titanium nitride and binder metals were prepared by the conventional ball-milling technique. Wet milling of the powders in acetone was performed in a Fritzsch Pullversette-5 centrifugal-type ball mill using 1.8×10^{-2} m diameter WC balls.

The ratio of feed to ball by mass was kept at 1:3. The additive nitride powder, i.e. TiN, was initially milled with binder powders for 8 h followed by WC addition with an additional 28 h wet milling. 4 h before the completion of milling, 2 wt% micronized wax powder was added to the charge. After the milling

0022–2461

TABLE I Characteristics of different powders

WC powder
Supplier: Widia (India) Ltd
Average particle size: 3.2 μm (FSSS)
Total carbon: 6.12%
Free carbon: 0.10%

TiN powder
Supplier: H. C. Starck, FRG
Average particle size: 3–4 μm (FSSS)

Co powder
Supplier: H. C. Starck, FRG
Average particle size: 2.3 μm (FSSS)
Chemical analysis: Ni 0.20%, Fe 0.04%, O 3500 p.p.m., Co balance

Ni powder
Supplier: Inco (UK), Type 123
Average particle size: 3.7 μm (FSSS)
Chemical analysis: C 0.06%, Fe 0.005%, O 0.05%, Co 0.0003%, N_2 0.003%, S 0.0003%, other elements 0.001%, Ni balance

Mo_2C powder
Source: USSR make
Average particle size: 3–4 μm (FSSS)

operation, the wet powder slurry was dried in a vacuum oven. From the ball-milled powder premix rectangular green compacts of size 24.7 mm × 7.7 mm × 5.5 mm were prepared in a hydraulic compaction press at pressure range 350–450 MPa so as to obtain a constant green density (approximately 55 % of theoretical density) for all the compositions.

Dewaxing of the green samples was carried out in a silicon carbide resistance-heated tubular furnace for 2 h at 400 °C under a dry hydrogen or a 50 % H_2–50% N_2 mixture. The heating rate was maintained at about 2 °C min^{-1} to make sure that no damage was done to the green compacts during dewaxing. The dewaxed compacts so obtained were kept in a graphite boat packed with alumina powder and were subsequently sintered in the temperature range 1450–1500 °C (at intervals of 25 °C) for 1 h in dry hydrogen or 50% H_2–50% N_2 mixture, with the exception of straight WC–10Co hard metal which was sintered at 1425 °C in dry H_2 atmosphere only. The heating rate was around 8 °C min^{-1}. The hydrogen and nitrogen used were dried by passing through a Lectrodryer and Matheson 6406 gas purifier, respectively. The dew point of the hydrogen and nitrogen after such drying was − 35 °C. The optimum sintering temperature was found for different hard metal compositions by evaluating the sintered properties and by microstructural studies. Hot isostatic pressing of some of the selected alloys was carried out in Ar of 1000 bar pressure for 45 min at 1400 or 1450 °C in the production unit of a cemented carbide manufacturing plant.

The sintered densities were measured according to the following formula as suggested by Arthur [7] using the displacement method:

$$\text{Sintered density (g cm}^{-3}) = \frac{a}{b - c}$$

where a is the weight of the compact in air (g), b is the weight of xylene-impregnated compact in air (g) and c is the weight of xylene-impregnated compact in water (g).

The hardness of the sintered compacts was measured on a Vickers hardness testing machine model HPO 250 (Fritz Heckert, Leipzig) using a load of 30 kg. Five indentations were taken on each polished specimen, and the average value was determined.

The transverse rupture strength (TRS) of as-sintered specimens were determined under three-point loading according to ASTM specifications on an MTS machine with a crosshead speed of 0.2 mm min^{-1}. The maximum rupture load at the failure point of the test pieces was used in the following formula for calculating the TRS:

$$\text{TRS (MN m}^{-2}) = \frac{3PL}{2WT^2}$$

where P is the load (MN), L is the length (m), W is the width (m) and T is the thickness (m). For each set of specimens four tests were performed, and the average value was determined.

The indentation fracture toughness was measured according to the method followed by Shetty *et al.* [8, 9] based on Palmquivst crack geometry

$$K_c(\text{MN m}^{-3/2}) = \frac{0.0937P}{al^{1/2}}$$

where P is the indentation load (MN), a is the half indentation diagonal (m) and l is the Palmquivst crack length (m). Testing was carried out at a load of 60 kg using the Vickers hardness testing machine. Reproducibility in results required the removal of the subsurface damage which could persist after normal diamond lapping and polishing. This was achieved through doubling the duration of each lapping/polishing stage as suggested by Laugier [10]. Five indentations were taken on each sample, and the average values for indentation fracture toughness were determined.

Selected sintered compacts were wet-polished first on a cast-iron wheel using 7 μm diamond paste, followed by fine polishing by diamond pastes of

TABLE II Nominal composition of different alloys in volume and mass percentages

Alloy	Volume percentage					Mass percentage				
	Hard phase			Binder phase		Hard phase			Binder phase	
	WC	TiN	Mo_2C	Co	Ni	WC	TiN	Mo_2C	Co	Ni
A	83.6	–	–	16.4	–	90	–	–	10	–
B	63.0	20.0	–	17.0	–	79.3	8.7	–	12	–
C	63.0	20.0	–	8.5	8.5	79.3	8.7	–	6	6
D	63.1	17.4	2.5	8.5	8.5	78.7	7.5	1.8	6	6

decreasing grit size, namely 6, 2.5 and 1 μm. The unetched polished samples were observed under an optical microscope at a magnification of ×200 to get an idea of the pore size and distribution. The samples were finally etched by Murakami's reagent for 5–6 min.

SEM studies of polished as well as fractured samples were carried out on a Jeol 840A scanning electron microscope in secondary electron mode at an operating voltage of 20 kV. For SEM studies of the polished surface, the binder constituents of the samples were deep-electroetched by using 5% HCl solution at a potential difference of 3 V for 20 s.

Magnetic properties like coercivity and magnetic saturation were measured to get an idea of the binder phase distribution in the sintered hard metals. A Foester coercivity meter was used for this purpose.

3. Results

3.1. Liquid-phase sintered alloys

3.1.1. Sintered density and pore distribution

Fig. 1a shows the densification behaviour of different alloys studied, from which it is evident that WC–10Co hard metal achieved the full density at a sintering temperature of 1425 °C in a hydrogen atmosphere. Introduction of TiN into the system resulted in a high sintered porosity. A further increase in sintered porosity was observed when cobalt was partially substituted by nickel. Incorporation of Mo_2C along with cobalt–nickel binder improved the densification behaviour marginally as compared to that of the non-nickel-containing one. However, a great improvement in sintered density for all the compositions is evident (Fig. 1a) when the sintering atmosphere was changed to H_2–N_2 mixture from straight H_2. Even in an H_2–N_2 atmosphere, the maximum density obtained was about 97% of the theoretical density. No further improvement in sintered density was observed after 1475 °C sintering.

The pore morphology and distribution in sintered compacts of different compositions are presented in Fig. 2. A reduction in pore size and a better distribution of pores were observed when the sintering atmosphere was changed to H_2–N_2 mixture from straight H_2 (Fig. 2b). Partial substitution of cobalt by nickel resulted in an increase in both the porosity and the density of large pores. Addition of Mo_2C resulted in

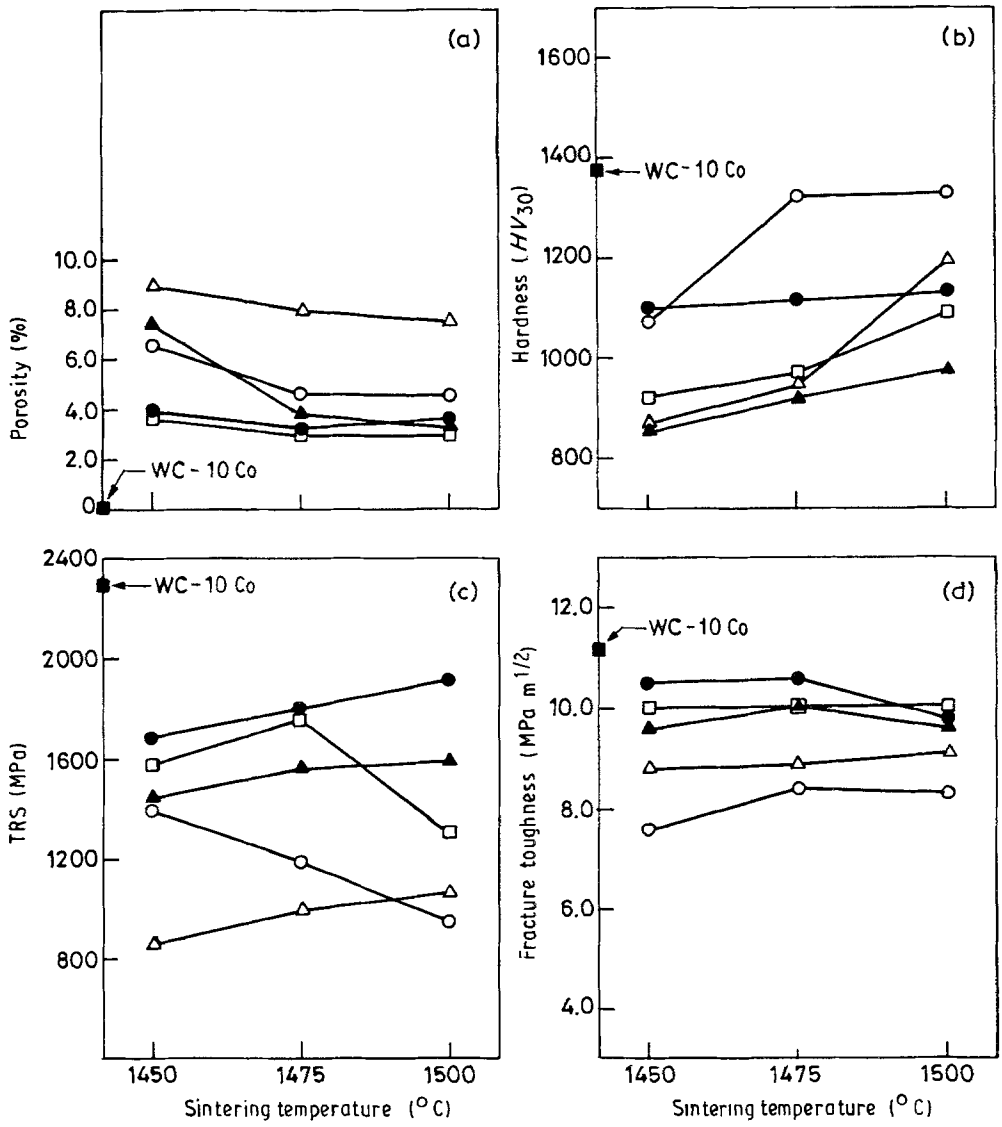

Figure 1 Effect of sintering temperature and atmosphere on properties of various hard metals: (a) sintered porosity, (b) Vickers hardness, (c) TRS, (d) indentation fracture toughness. (○) WC–8.7TiN–12Co, H_2; (●) WC–8.7TiN–12Co, H_2–N_2; (△) WC–8.7TiN–6Co–6Ni, H_2; (▲) WC–8.7TiN–6Co–6Ni, H_2–N_2; (□) WC–7.5TiN–1.8Mo_2C–6Co–6Ni, H_2–N_2.

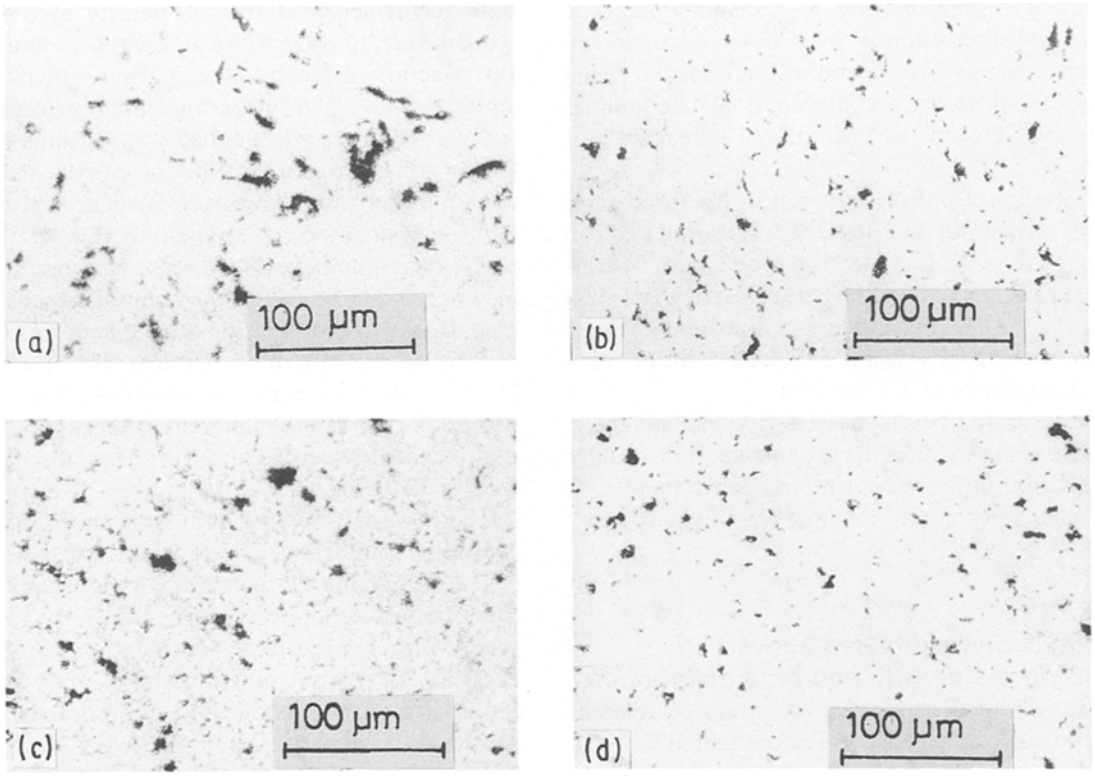

Figure 2 Microstructures of unetched specimens showing sintered porosity and their distribution: (a) WC–8.7TiN–12Co sintered in H_2, (b) WC–8.7TiN–12Co sintered in H_2–N_2, (c) WC–8.7TiN–6Co–6Ni sintered in H_2–N_2, (d) WC–7.5TiN–1.8Mo_2C–6Co–6Ni sintered in H_2–N_2 (all sintered at 1475 °C for 1 h).

a decrease in pore size and its better distribution (Fig. 2d) as compared to that of the previous composition (Fig. 2c). However, the pore size and its distribution for this particular composition are similar to that of the non-nickel-containing one (Fig. 2b and d).

3.1.2. Hardness

Hardness values did not show much change when TiN was introduced in WC–10Co hard metal (Fig. 1b), but the partial substitution of cobalt by nickel in WC–8.7TiN–12Co composition decreased the hardness to a great extent. A further decrease in hardness value was observed when sintering was carried out in H_2–N_2 mixture. The hardness value improved only marginally when Mo_2C was incorporated in the system along with cobalt–nickel binder. The values showed an increasing trend with increase in sintering temperature, except for the WC–8.7TiN–12Co composition which did not show any change after 1475 °C sintering temperature.

3.1.3. Transverse rupture strength

The TRS value obtained for any composition containing TiN was much less than that of WC–10Co hard metal (Fig. 1c). A drastic drop in TRS was observed in WC–8.7TiN–12Co hard metal when sintered in H_2. Partial substitution of cobalt by nickel further decreased the TRS. The change in TRS values due to the change in sintering atmosphere to H_2–N_2 mixture was encouraging. Much improvement was observed in both WC–8.7TiN–12Co and WC–8.7TiN–6Co–6Ni compositions. The presence of molybdenum in the binder phase of WC–7.5TiN–1.8Mo_2C–6Co–6Ni hard metal brought up the TRS value to the level of WC–8.7TiN–12Co composition when sintered at 1475 °C in H_2–N_2 mixture. The TRS value of WC–8.7TiN–12Co decreased sharply with increase in sintering temperature, but just the reverse trend was observed in the case of WC–8.7TiN–6Co–6Ni composition. However, in H_2–N_2 mixture sintering the TRS values increased with increase in temperature except for WC–7.5TiN–1.8Mo_2C–6Co–6Ni which showed a decrease after 1475 °C.

3.1.4. Indentation fracture toughness

Fracture toughness results (Fig. 1d) followed almost the same trend as that of the TRS. The introduction of TiN into WC–10Co hard metal greatly decreased the toughness value. A marginal improvement was observed when cobalt binder in the WC–8.7TiN–12Co composition was partially substituted by nickel. Fracture toughness values for all the compositions, as for the TRS variation, greatly increased when the sintering atmosphere was changed to H_2–N_2 mixture. The change in toughness values with increase in sintering temperature was similar to that of TRS variation.

3.1.5. Magnetic properties

Introduction of TiN in WC–10Co hard metal resulted in an increase in coercivity, whereas the partial substitution of cobalt by nickel in WC–8.7TiN–12Co composition decreased the coercivity (Fig. 3a). However,

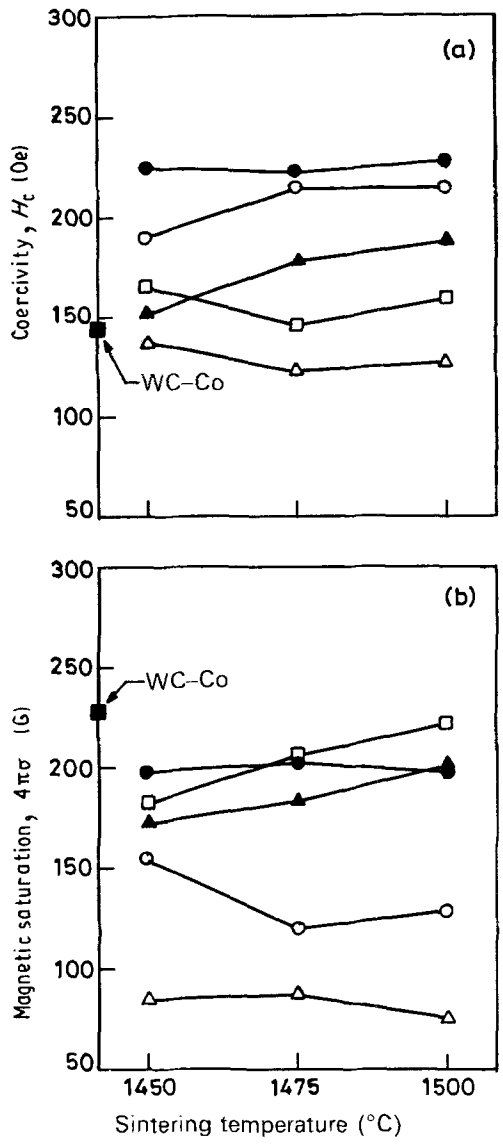

Figure 3 Magnetic property variations of different hard metals with sintering temperature: (a) coercivity, (b) magnetic saturation. (○) WC–8.7TiN–12Co, H_2; (●) WC–8.7TiN–12Co, H_2–N_2; (△) WC–8.7TiN–6Co–6Ni, H_2; (▲) WC–8.7TiN–6Co–6Ni, H_2–N_2; (□) WC–7.5TiN–1.8Mo_2C–6Co–6Ni, H_2–N_2.

the change of sintering atmosphere from straight H_2 to H_2–N_2 mixture resulted in an increase in coercivity for both the compositions. Incorporation of Mo_2C in the system with cobalt–nickel binder brought down the value to that of straight WC–10Co hard metal.

Fig. 3b shows the magnetic saturation variation of different hard metals. Magnetic saturation values obtained in all the compositions were higher when sintered in H_2–N_2 mixture as compared to those sintered in straight H_2. Introduction of TiN resulted in a drop in magnetic saturation value. A further decrease was observed when cobalt was partially substituted by nickel. However, Mo_2C addition increased the magnetic saturation and maintained the same level as to that of WC–10Co hard metal. Magnetic saturation values decreased with increase in sintering temperature when alloys were sintered in H_2, but in H_2–N_2 mixture it either remained constant or increased with increase in sintering temperature.

3.1.6. Microstructure

Although not much detailed information could be gathered from the optical microstructures (Fig. 4), careful observation reveals that the partial substitution of cobalt by nickel resulted in grain coarsening. Incorporation of Mo_2C in WC–8.7TiN–6Co–6Ni hard metal resulted in a cored microstructure (Fig. 4f). The microstructure also reveals a better grain size uniformity as compared with the WC–8.7TiN–6Co–6Ni composition.

SEM micrographs (Fig. 5) confirm the observations obtained from the optical micrographs and reveal finer details. From Fig. 5d and e it is clearly evident that the partial substitution of cobalt by nickel in WC–8.7TiN–12Co resulted in grain coarsening, specifically leading to large TiN grains. Addition of Mo_2C helped in producing a better microstructure as far as the uniformity in grain size was concerned. Not much difference was observed between the microstructure of this particular composition (Fig. 5f) and WC–8.7TiN–12Co (Fig. 5c).

3.1.7. SEM fractographs

Fracture surfaces of all the compositions show the presence of porosity (Fig. 6). Cracks must have initiated from large pores resulting in catastrophic failure. The grain coarsening effect due to partial substitution of cobalt by nickel can be seen on the fracture surface (Fig. 6d and e). Though not much difference was observed in SEM micrographs between WC–8.7TiN–12Co (Fig. 5c) and WC–7.5TiN–1.8Mo_2C–6Co–6Ni (Fig. 5f), a clear difference can be noticed on the fracture surfaces. The latter composition shows a better uniformity of grain size as compared to the former. Secondly, the former shows a dimpled binder phase along with fractured TiN/WC particles, whereas the latter shows mostly tear ridges of binder phase and smooth carbide/nitride particles. The hard metals sintered in H_2–N_2 mixture show more dimpled structure on the fracture surface.

3.2. Hot isostatically pressed alloys

Table III shows the mechanical properties of HIPed hard metals. The percentage increase in sintered properties of different hard metals after HIP with respect to as-sintered ones is presented in Fig. 7. Nearly full density with residual porosity in the range of 0.10–0.15% was achieved when HIP was done at 1450 °C. From Table III it is evident that HIP resulted in a great enhancement in all the investigated mechanical properties. The only exception is the fracture toughness values obtained after HIP at 1400 °C, which show a decrease.

The pore size and distribution in the HIPed hard metals are shown in Fig. 8. Large pores in the as-sintered compacts were eliminated by HIP. The pore size is rather small and they have a better distribution in WC–8.7TiN–12Co hard metal than those of WC–7.5TiN–1.8Mo_2C–6Co–6Ni composition.

Fig. 9 shows optical microstructures of hard metals HIPed at 1400 and 1450 °C. An increase in HIP temperature from 1400 to 1450 °C resulted in grain coarsening. However, the average grain size of

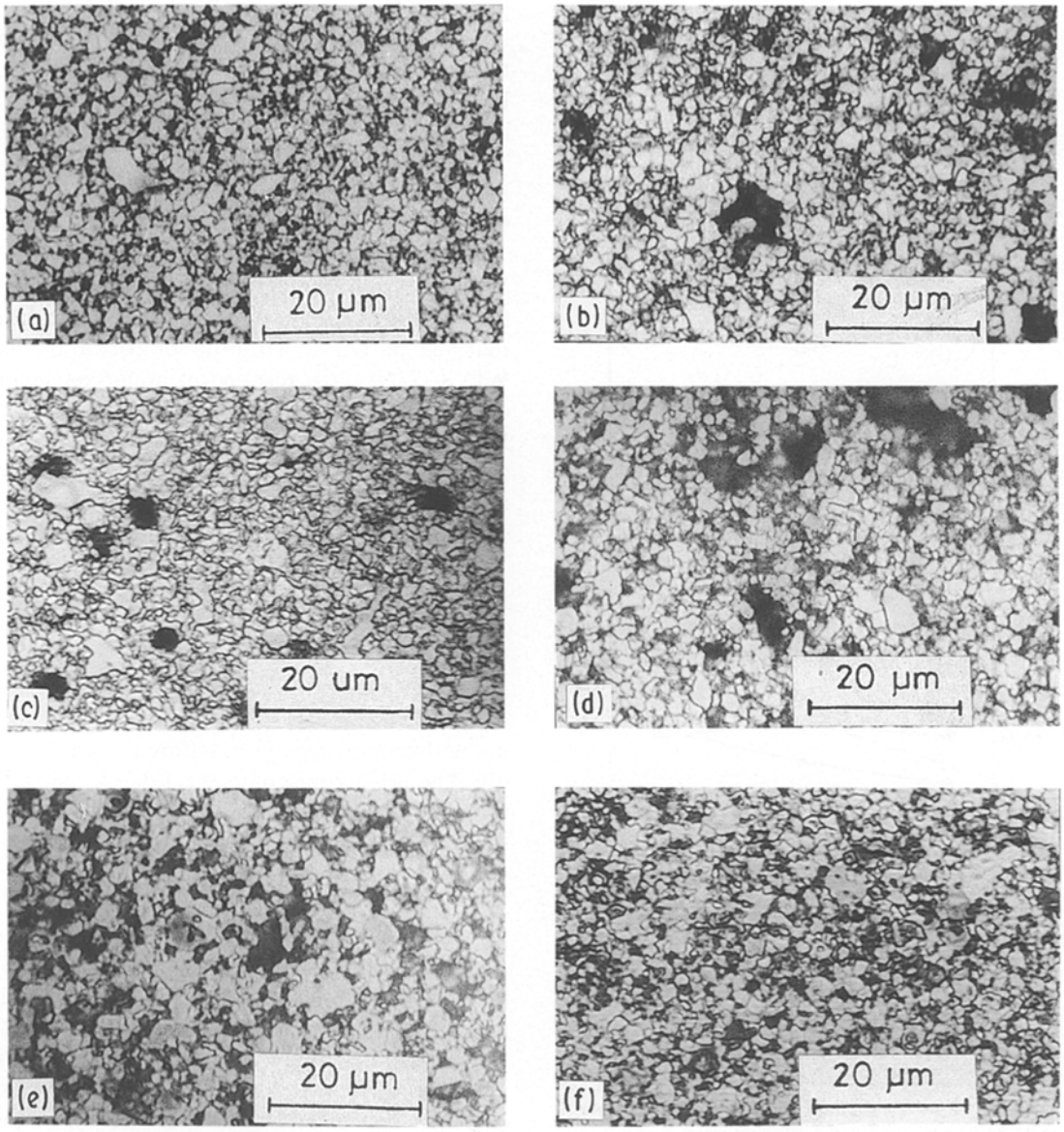

Figure 4 Optical microstructures of hard metals: (a) WC–10Co sintered in H_2, (b) WC–8.7TiN–12Co sintered in H_2, (c) WC–8.7TiN–12Co sintered in H_2–N_2, (d) WC–8.7TiN–6Co–6Ni sintered in H_2, (e) WC–8.7TiN–6Co–6Ni sintered in H_2–N_2, (f) WC–7.5TiN–1.8Mo_2C–6Co–6Ni sintered in H_2–N_2; (a) sintered at 1425 °C, (b)–(f) sintered at 1475 °C for 1 h.

WC–7.5TiN–1.8Mo_2C–6Co–6Ni hard metal is relatively smaller than that of WC–8.7TiN–12Co. These observations are further confirmed by the SEM microstructures presented in Fig. 10.

The differences between the fracture surfaces of as-sintered hard metals (Fig. 6) and HIPed ones (Fig. 11) are clear. Fig. 6 shows that crack initiation takes place mainly from large pores, whereas in Fig. 11 large carbide/nitride particles are the crack initiators. The cleavage structure of large carbide/nitride particles is more pronounced in WC–8.7TiN–12Co than in the case of WC–7.5TiN–1.8Mo_2C–6Co–6Ni.

4. Discussion

4.1. Liquid-phase sintered alloys

Hard metals are typical examples of systems undergoing liquid-phase sintering during powder metallurgy P/M processing. The required liquid phase results from the formation of a eutectic at the sintering temperature. From a technical point of view, liquid-phase sintering is very attractive as it provides faster sintering and complete densification without the need for any external pressure. Higher sinterability is due to the enhanced atomic diffusion in the presence of a liquid phase which ultimately facilitates material transport. In hard metal systems, where the higher-melting phase is the harder phase, liquid-phase sintering results in a two-phase composite material with ductile behaviour in spite of a large quantity of hard phase. The minimum criteria for successful liquid-phase sintering are (i) a low-temperature liquid, (ii) solubility of solid in liquid, and (iii) liquid wetting of the solid grains [11]. In the WC–Co system the liquid phase produced during sintering satisfies all the three basic conditions mentioned above.

The end properties of hard metals are derived from those of their respective constituents. The different microstructures resulting from a combination of hard phase and binder phase naturally have an effect on the sintered properties. On the other hand, the microstructure developed at the time of sintering is largely

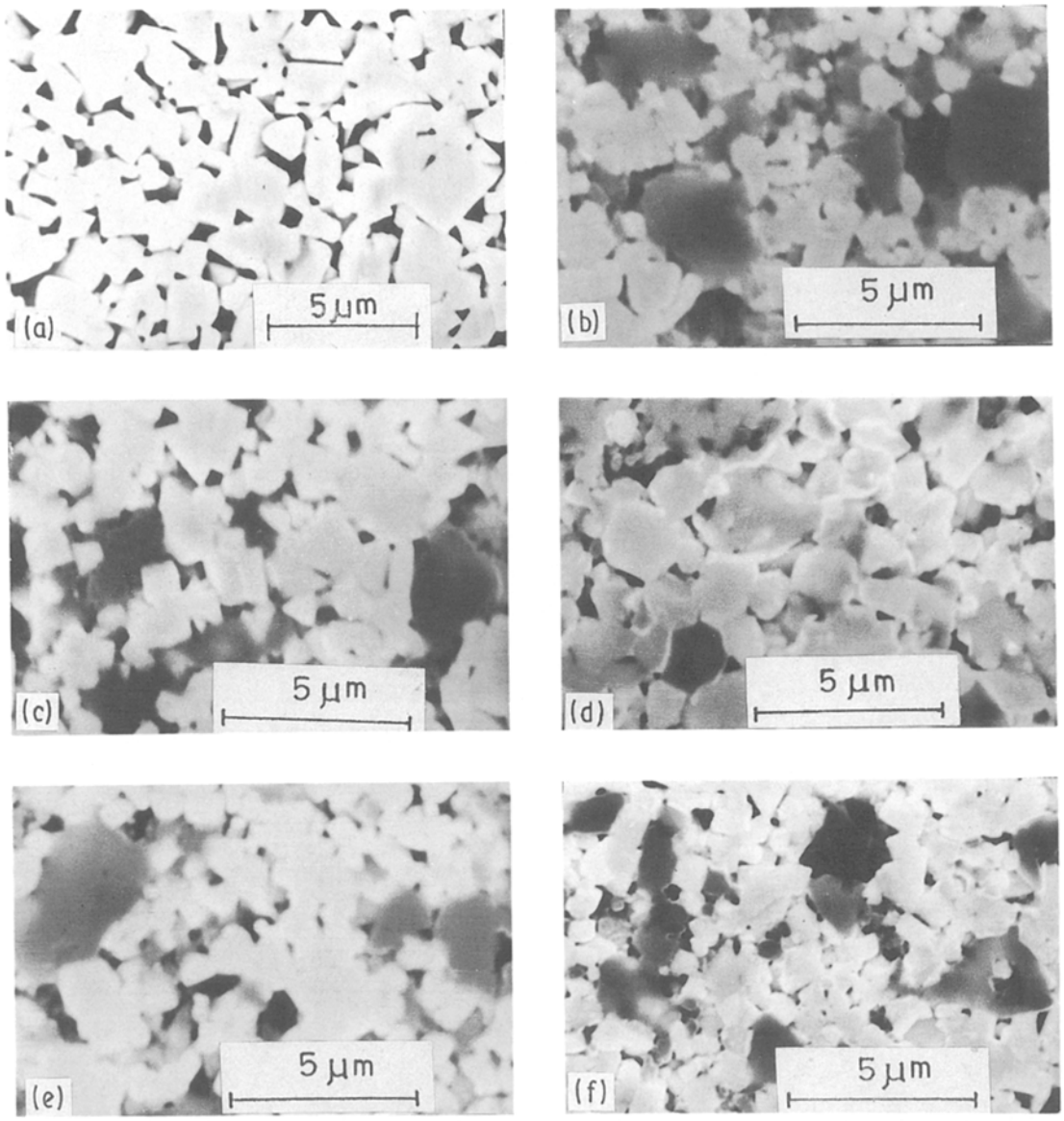

Figure 5 SEM microstructures of hard metals: (a) WC–10Co sintered in H_2, (b) WC–8.7TiN–12Co sintered in H_2, (c) WC–8.7TiN–12Co sintered in H_2–N_2, (d) WC–8.7TiN–6Co–6Ni sintered in H_2, (e) WC–8.7TiN–6Co–6Ni sintered in H_2–N_2, (f) WC–7.5TiN–1.8Mo_2C–6Co–6Ni sintered in H_2–N_2; (a) sintered at 1425 °C, (b)–(f) sintered at 1475 °C for 1 h.

dependent on the interaction between the hard phases and the binder phases.

The densification behaviour of hard metals during liquid-phase sintering is obviously related to the interfacial energy, i.e. the energy of the hard phase–binder phase interface and its relation to the grain boundary energy of the hard phase. In addition another feature of the interaction of hard phases with the binder phase is that their solubility in the melt plays an important role in hard-metal production [5]. WC has a higher solubility in cobalt than in nickel, whereas TiC/TiN/Ti(C, N) have a higher solubility in nickel than in cobalt. This suggests that a cobalt–nickel binder could be a reasonable compromise for hard metals containing both WC and TiN. The same explanation holds true for wettability as well.

The effectiveness of molybdenum addition in the nickel binder in promoting small grain size and improved mechanical properties of TiC/Ti(C, N)-based hard metals is well known [4, 5]. Recently Barranco and Warenchak [12] reported that molybdenum addition in nickel also improves the wettability of WC, which they explained on the basis of interfacial energy. Molybdenum forms a continuous series of solid solutions with tungsten and titanium. Molybdenum diffuses into WC/TiN/Ti(C, N) through the solid–liquid interface, which results in a lowering of the solid–liquid interfacial energy.

4.1.1. WC–10Co

From the results obtained it is apparent that the sintered properties of WC–10Co hard metal are comparable to those available in the literature [13].

4.1.2. WC–8.7TiN–12Co

Full density of the hard metal was not achieved even at a sintering temperature of 1500 °C, which may be related to the poor wettability of TiN by cobalt [14]. However, though complete elimination of porosity was not possible in normal sintering, a better densification was observed when alloys were sintered in H_2–N_2 mixture as compared to straight H_2. The

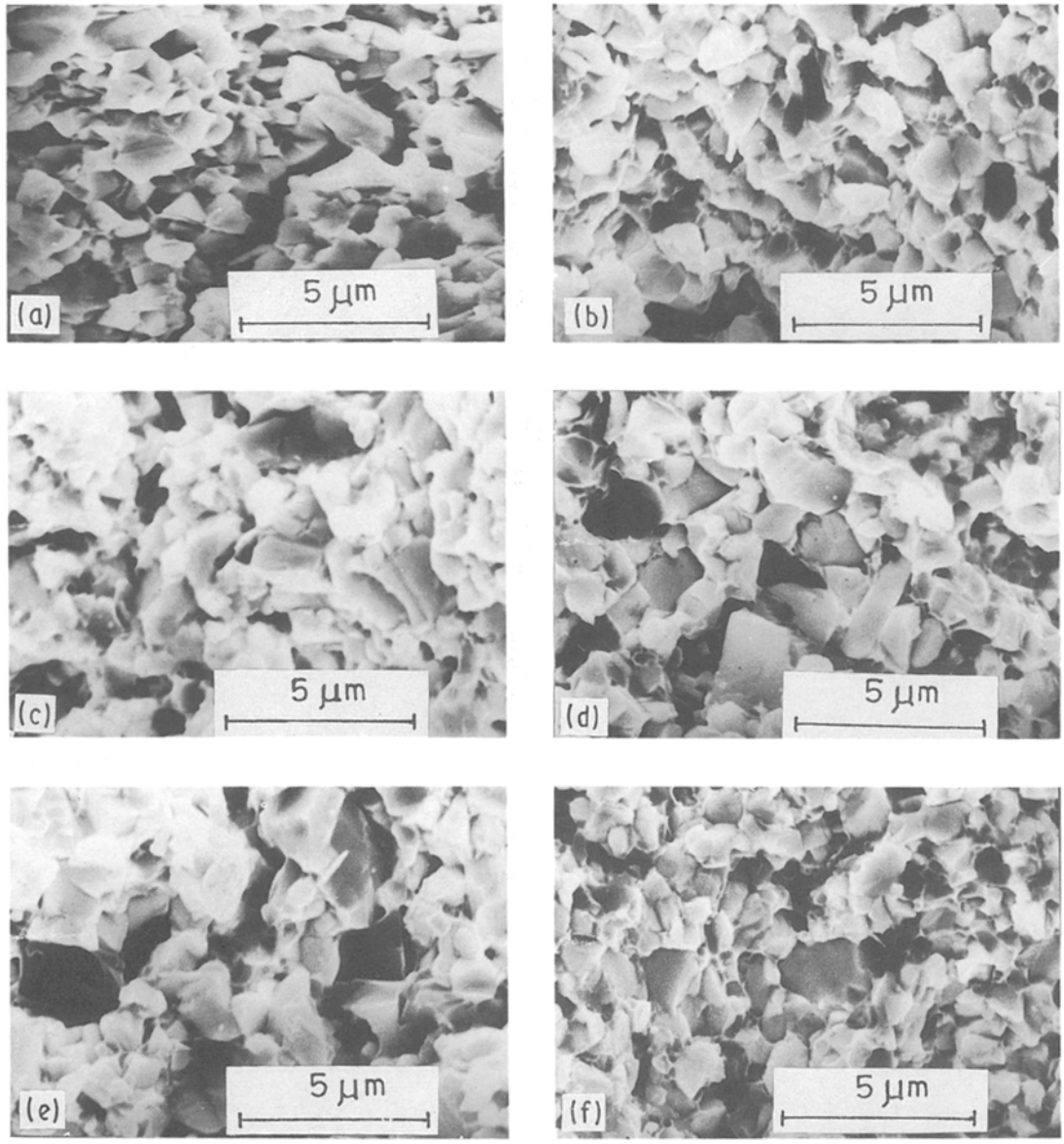

Figure 6 SEM fractographs of hard metals: (a) WC–10Co sintered in H_2, (b) WC–8.7TiN–12Co sintered in H_2, (c) WC–8.7TiN–12Co sintered in H_2–N_2, (d) WC–8.7TiN–6Co–6Ni sintered in H_2, (e) WC–8.7TiN–6Co–6Ni sintered in H_2–N_2, (f) WC–7.5TiN–1.8Mo_2C–6Co–6Ni sintered in H_2–N_2; (a) sintered at 1425 °C, (b)–(f) sintered at 1475 °C for 1 h.

literature on TiN/Ti(C, N) [4, 15] reveals that their sintering cannot be done in a dynamic vacuum or in H_2 because of the evolution of nitrogen and the resulting decomposition of TiN/Ti(C, N). It appears that this has occurred in the present alloys as well. Such a feature diminishes the carbon content from WC, thus facilitating η-phase formation. η-phase formation involves the consumption of cobalt which otherwise produces liquid at the sintering temperature. Secondly, depletion of carbon in the alloy reduces the fluidity of the liquid melt present during sintering. These effects ultimately lead to a higher sintered porosity in the hard metal sintered in H_2.

As far as the microstructural changes are concerned, not much difference is observed between this particular composition and WC–10Co hard metal except for the presence of pores in the former. From the microstructure it is also evident that no alloying of WC and TiN took place. This could be attributed to the fact that WC is stable in N_2 even at high temperatures [16] and does not form a solid solution with TiN during sintering.

Mechanical properties, namely hardness, TRS and fracture toughness values, are much lower than those of the WC–10Co composition. This is basically because of the presence of porosity in the structure. It is clearly evident from the fracture surface (Fig. 6) that crack initiation invariably starts from large pores or voids, resulting in catastrophic failure. However, when the sintering atmosphere was changed to H_2–N_2 mixture, in spite of having a large amount of porosity the mechanical properties were enhanced, except for the hardness which decreased. This can be explained on the basis of a hard and brittle η-phase present in the structure after H_2 sintering. This fact is further confirmed by magnetic saturation values (Fig. 3b) which drop sharply when there is any η-phase present in the structure. This is attributed to the reduction in the amount of magnetic phase when cobalt is incorporated in the non-magnetic η-phase [17].

TABLE III Sintered porosity and mechanical properties of TiN-containing hard metals in as-sintered and HIPed conditions

Composition hard metal	Porosity (%)			Hardness (HV_{30})			Transverse rupture strength (MPa)			Fracture toughness (MPa $m^{1/2}$)		
	Sintered[a]	HIPed[b]		Sintered	HIPed		Sintered	HIPed		Sintered	HIPed	
		1400 °C	1450 °C		1400 °C	1450 °C		1400 °C	1450 °C		1400 °C	1450 °C
WC–8.7TiN–12Co	3.64	0.41	0.15	1112	1238	1268	1795	1940	2285	10.57	9.48	10.78
WC–7.5TiN–1.8Mo_2C–6Co–6Ni	3.25	0.30	0.10	958	1265	1285	1770	1837	2155	10.02	9.34	10.63

[a] Sintered at 1475 °C for 60 min in $N_2 + H_2$ (50:50).
[b] HIPed in argon atmosphere at a pressure of 1000 bar (soak time 45 min).

It was not possible to isolate the effect of microstructural changes due to the presence of porosity on the mechanical behaviour after TiN addition.

4.1.3. WC–8.7TiN–6Co–6Ni

Partial substitution of cobalt by nickel did not improve the densification behaviour for WC–8.7TiN–6Co–6Ni composition. TiN has a better wettability in nickel than in cobalt, whereas it is the other way round for WC. It appears from the present results related to densification, pore morphology and its distribution that the overall wettability deteriorates due to the binder phase modification. The grain coarsening effect observed is thus in consonance with the changes in wettability as explained above.

The deterioration of mechanical properties when nickel was introduced in the previous hard metal composition can be attributed to a higher sintered porosity and coarser microstructure, as compared with the WC–8.7TiN–12Co composition.

The improvements in densification and mechanical properties due to a change in sintering atmosphere from straight H_2 to H_2–N_2 mixture are because of the same reasons as explained in the previous section. However, though the microstructure in the latter case is free of η-phase, the magnetic saturation value obtained is less than that of WC–8.7TiN–12Co. This may be due to the fact that the introduction of nickel into the cobalt binder metal leads to the presence of some free carbon in the system, and even a slightly decarburized hard metal shows a lowering of both magnetic saturation and coercivity values [18].

4.1.4. WC–7.5TiN–1.8Mo_2C–6Co–6Ni

As reported in the literature [4, 12] the presence of molybdenum in the nickel binder improves its wettability with both WC and TiN. This contributes to the achievement of a better densification behaviour in the present composition. Unlike the previous two compositions, in this particular composition a cored microstructure is observed. Since molybdenum forms a continuous series of solid solutions with tungsten and titanium, alloying of WC–Mo_2C and TiN–Mo_2C took place to form (W, Mo)C and (Ti, Mo) (C, N) solid solutions, respectively, which gave rise to a cored microstructure (Fig. 4f). However, at the same time the improved wettability resulted in a uniform grain size distribution.

Incorporation of Mo_2C in WC–8.7TiN–6Co–6Ni resulted in an enhancement of mechanical properties. The relatively high hardness and TRS of the present hard metal can be explained on the basis of an improved wettability of WC and TiN by the binder phase, less sintered porosity, and uniformity in grain size distribution.

4.2. Hot isostatically pressed alloys

It is virtually impossible by normal liquid-phase sintering to achieve a fully dense product out of TiN/Ti(C, N)-based hard metals, irrespective of any

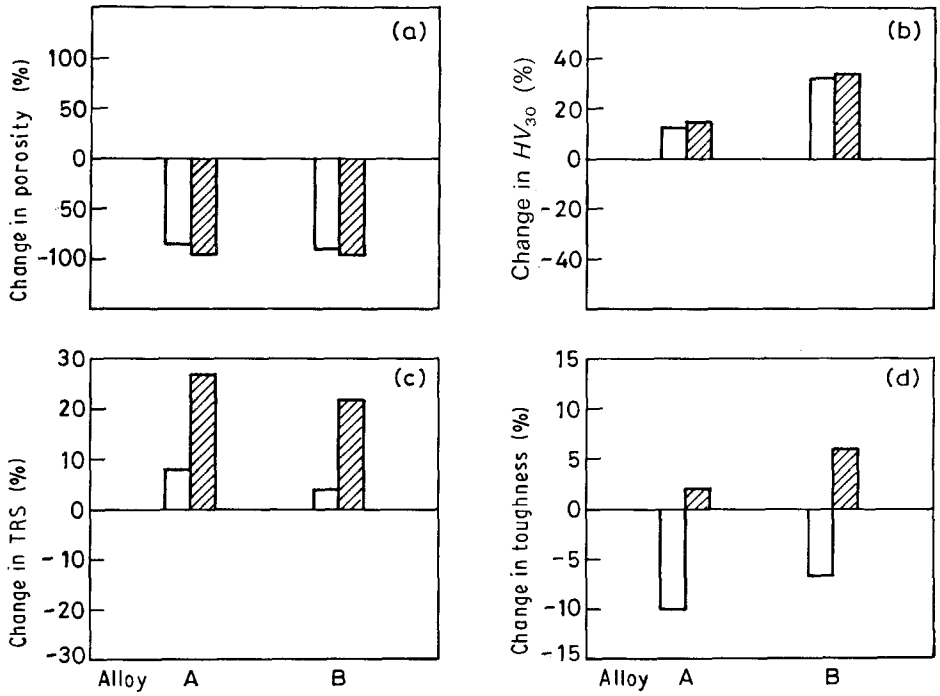

Figure 7 Percentage changes in porosity and mechanical properties of hard metals after HIP with respect to the corresponding properties of liquid-phase sintered hard metals (sintered at 1475 °C in H_2–N_2): (a) sintered porosity, (b) Vickers hardness, (c) TRS, (d) indentation fracture toughness. Alloy A: WC–8.7TiN–12Co, alloy B: WC–7.5TiN–1.8Mo_2C–6Co–6Ni. Clear bars: HIPed at 1400 °C, shaded bars: HIPed at 1450 °C.

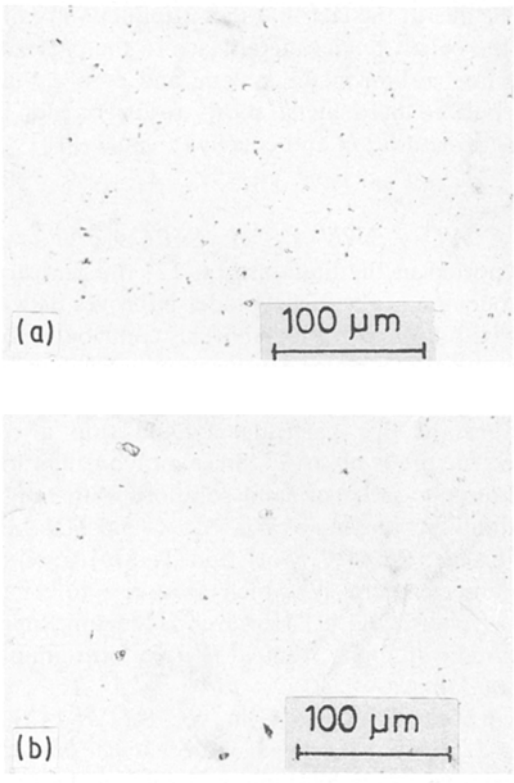

Figure 8 Microstructures of unetched hard metals HIPed at 1450 °C showing residual porosity and its distribution: (a) WC–8.7TiN–12Co, (b) WC–7.5TiN–1.8Mo_2C–6Co–6Ni.

variation in the sintering atmosphere. This may arise from the fact that pores containing nitrogen gas arising out of denitrification or the sintering atmosphere are difficult to remove during sintering and invariably give rise to large pores in the sintered compacts [4, 15]. These pores are the origin of fractures and are responsible for the low strength of such hard metals. HIP of such liquid-phase sintered compacts seems an obvious way of eliminating such defects and achieving increased strength.

Since it was not possible to achieve fully density in the present series of hard metal compositions by liquid-phase sintering alone, it was decided to apply HIP to some of the sintered alloys. As mentioned in Section 4.1, the partial substitution of cobalt binder by nickel resulted in relatively higher sintered porosity, non-uniform microstructure, and poor mechanical properties, and hence further processing through the HIP route of WC–8.7TiN–6Co–6Ni was not tried out.

HIP treatment after sintering was effective for eliminating large pores, though some small pores were still left. HIP at 1400 °C gave rise to some laminated pores on voids in the compacts. This could be attributed to the fact that liquid-phase sintering resulted in a continuous hard-phase skeleton, and in subsequent HIP at 1400 °C the contributions of power-law creep/plastic deformation and the amount of liquid phase were not sufficient to eliminate the large pores completely. However, such a feature was absent when HIP was carried out at 1450 °C.

In as-sintered hard metals, large pores were the origin of fractures. The strength of such processed hard metals was closely related to the size and type of defect. The strength and toughness of such hard metals were greatly enhanced when these defects were eliminated by HIP treatment which eliminated the large pores, but consequently gave rise to a relatively coarse-grained structure. However, it appears that the beneficial contribution of eliminating the large pores is much more than the effect of grain

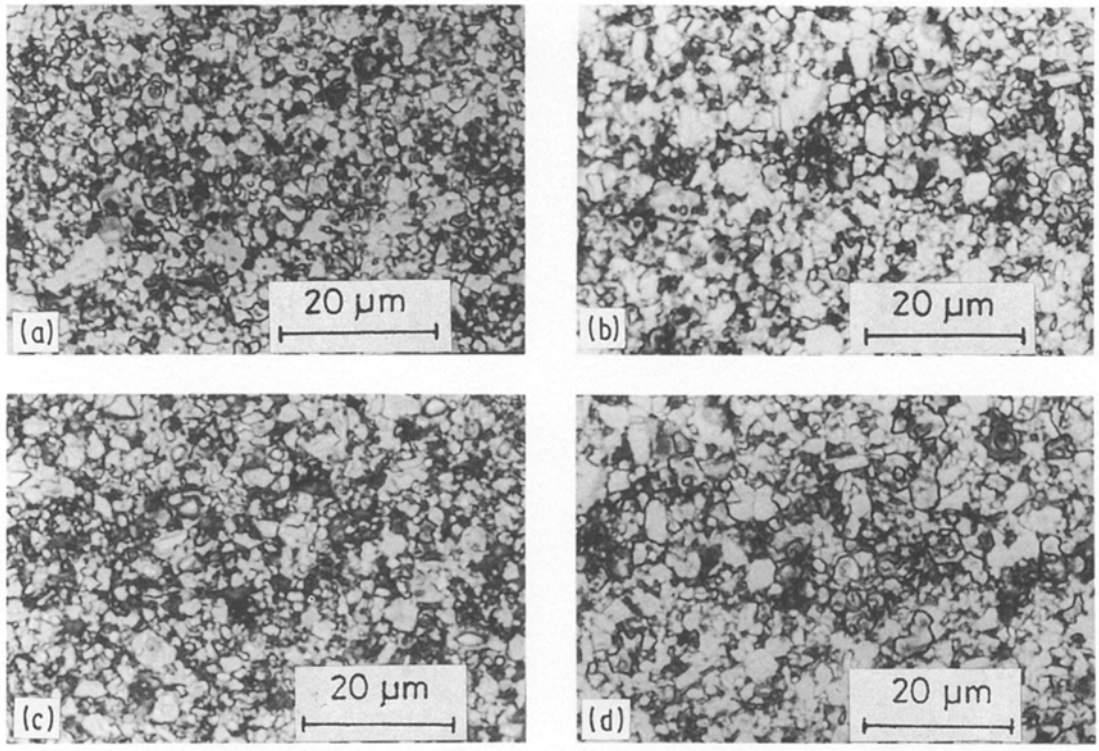

Figure 9 Optical microstructures of HIPed hard metals: (a) WC–8.7TiN–12Co HIPed at 1400 °C, (b) WC–8.7TiN–12Co HIPed at 1450 °C, (c) WC–7.5TiN–1.8Mo_2C–6Co–6Ni HIPed at 1400 °C, (d) WC–7.5TiN–1.8Mo_2C–6Co–6Ni HIPed at 1450 °C.

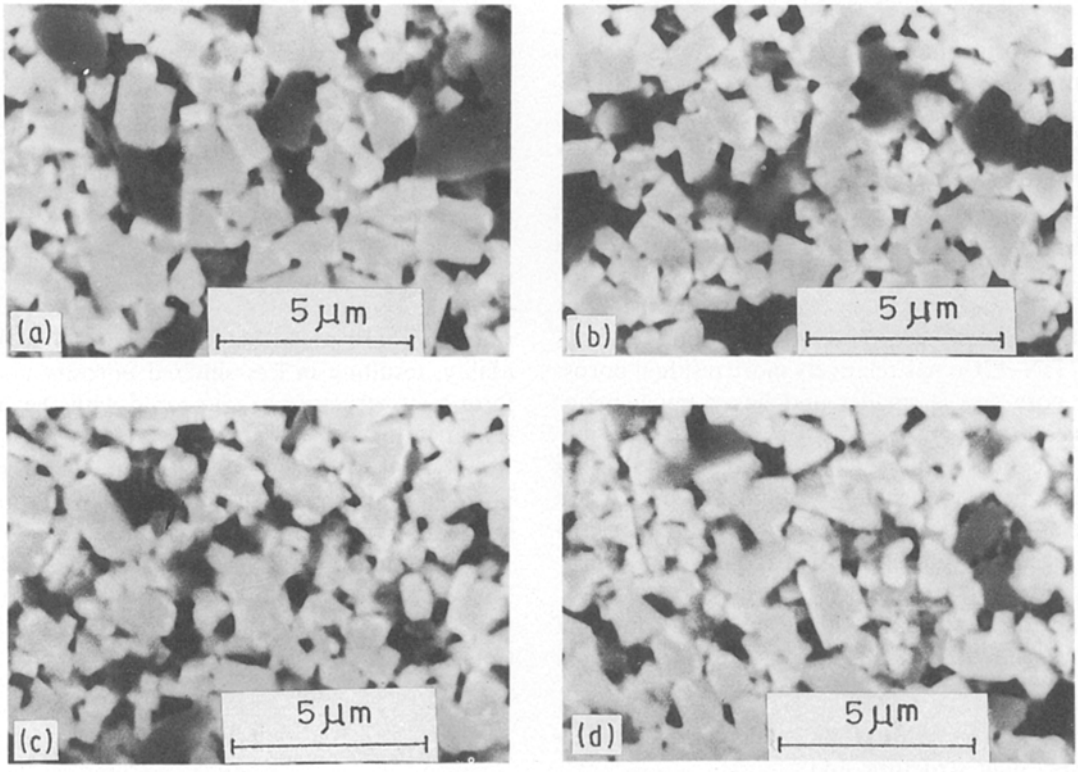

Figure 10 SEM microstructures of HIPed hard metals: (a) WC–8.7TiN–12Co HIPed at 1400 °C, (b) WC–8.7TiN–12Co HIPed at 1450 °C, (c) WC–7.5TiN–1.8Mo_2C–6Co–6Ni HIPed at 1400 °C, (d) WC–7.5TiN–1.8Mo_2C–6Co–6Ni HIPed at 1450 °C.

coarsening on the mechanical properties. The strength improvement is thus mainly due to the decrease in defect size. The noticeable feature in such HIPed alloys is the decrease in toughness values when HIPed at 1400 °C. As mentioned earlier, the hard metal HIPed at 1400 °C contained laminated defects having sharp edges, such that the stress concentration at these edges was much more than at normal pores. As a result, when these edges interact with any propagating crack they open up very easily. On the other hand, the hard metals HIPed at 1450 °C have an improved toughness, since they do not have such defects.

Coming to the individual hard metal compositions, WC–7.5TiN–1.8Mo_2C–6Co–6Ni exhibited less

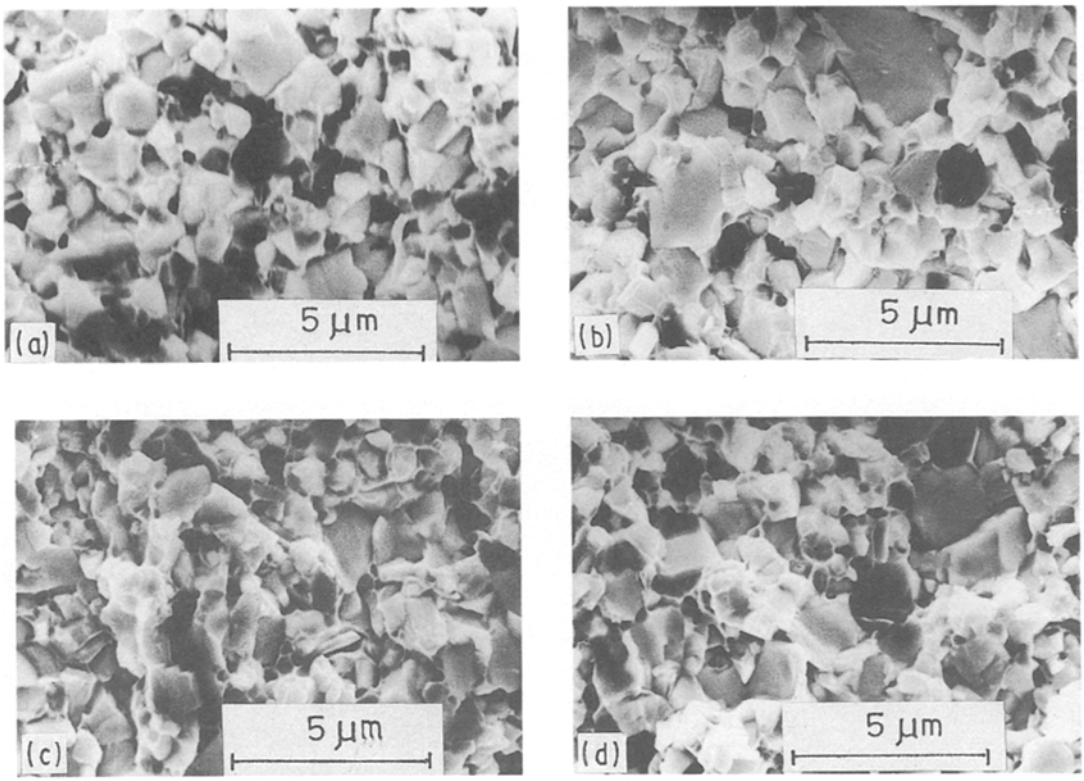

Figure 11 SEM fractographs of HIPed hard metals: (a) WC–8.7TiN–12Co HIPed at 1400 °C, (b) WC–8.7TiN–12Co HIPed at 1450 °C, (c) WC–7.5TiN–1.8Mo_2C–6Co–6Ni HIPed at 1400 °C, (d) WC–7.5TiN–1.8Mo_2C–6Co–6Ni HIPed at 1450 °C.

residual porosity and relatively lower average grain size than WC–8.7TiN–12Co. As far as the SEM fractographs are concerned, there is not much difference with the exception that the WC–8.7TiN–12Co alloy contained more transgranularly fractured WC/TiN particles than the WC–7.5TiN–1.8Mo_2C–6Co–6Ni composition. According to this the latter hard metal should have a better TRS and toughness, but the reverse is true. This can be explained on the basis of residual pore size and distribution. Though WC–8.7TiN–12Co has relatively more residual porosity, the pore size is smaller and has a much better distribution as compared with the WC–7.5TiN–1.8Mo_2C–6Co–6Ni alloy. The present result also explains that below a certain size limit, the defects are not critical in determining the strength of the hard metal. In general, the defect size is related to the hard-phase grain size.

The hardness variation, however, shows just the opposite trend to that of TRS or toughness, which may be attributed to the following facts:

(i) WC–7.5TiN–1.8Mo_2C–6Co–6Ni hard metal has a relatively finer structure; and

(ii) (W, Mo)C and (Ti, Mo) (C, N) solid solutions are harder than WC and TiN, respectively.

5. Conclusions

The following conclusions can be drawn, based on the results of the hard metals investigated:

1. The addition of TiN resulted in a high sintered porosity and deteriorated the mechanical properties to a great extent.

2. Sintering experiments showed that sintering in H_2 resulted in denitrification of TiN and thus an H_2–N_2 (50:50) atmosphere was a better proposition.

3. No alloying of WC and TiN took place during sintering.

4. Partial substitution of cobalt in WC–8.7TiN–12Co resulted in increased sintered porosity and non-uniform microstructure.

5. Incorporation of Mo_2C in WC–8.7TiN–6Co–6Ni hard metal helped in improving the wettability, resulting in less sintered porosity and a uniform microstructure as compared with the composition mentioned in (4) above.

6. HIP treatment was effective in eliminating large pores in liquid-phase sintered alloys and greatly enhanced the mechanical properties.

7. Among all the investigated HIPed hard metals, WC–8.7TiN–12Co exhibited equivalent properties to that of WC–10Co processed through liquid-phase sintering.

References

1. N. TSCHIYA, O. TERADA, A. SASAKI and H. SUZUKI, *J. Jap. Soc. Powd. Powd. Met.* **37** (1990) 80.
2. L. PRAKASH, Report Kfk-Ext. 6/78-1 (1978) 87 (Kerufors-chungszentrum Karlsruhe GmbH).
3. G. S. UPADHYAYA and S. K. BHAUMIK, *Mater. Sci. Eng. A.* **105/106** (1988) 249.
4. R. KIEFFER, P. ETTMAYER and M. FREUDHOFMEIER, in "Modern Development in P/M", Vol. 5, edited by H. H. Hausner (Plenum, New York, 1971) p. 201.
5. H. E. EXNER, *Int. Met. Rev.* **24** (1979) 149.
6. Y. TANIGUCHI, K. SASAKI, M. VEKI and K. KOBORI, *Int. J. Refrac. Hard Met.* **5** (September 1986) 171.
7. G. ARTHUR, *J. Inst. Metals* **83** (1954) 1329.

8. D. K. SHETTY, I. G. WRIGHT, P. N. MINCER and A. H. CLAUER, *J. Mater. Sci.* **20** (1980) 1873.
9. C. B. PONTON and R. D. RAWLINGS, *Mater. Sci. Tech.* **5** (1989) 961.
10. M. T. LAUGIER, *Ceram. Int.* **15** (1989) 121.
11. R. M. GERMAN, "Liquid Phase Sintering" (Plenum, New York, 1985) p. 43.
12. J. M. BARRANCO and R. A. WARENCHAK, *Int. J. Refrac. Hard Met.* **8** (June 1989) 102.
13. V. K. SARIN, in "Advances in Powder Technology", edited by G. Y. Chin (ASM, Ohio, 1982) p. 253.
14. P. S. KISLEY (ed.), in "Kermeti" (Naukova Dumka, Kiev, 1985) p. 159 (in Russian).
15. P. S. KISLY and M. A. KUZENKOVA, *Powd. Met. Int.* **4** (1972) 67.
16. L. E. TOTH, "Transition Metal Carbides and Nitrides" (Academic, New York, 1977) p. 85.
17. J. FRETAG and H. E. EXNER, in "Modern Development in P/M", Vol. 10, edited by H. H. Hausner and P. W. Taubenblat (Metal Powder Industries Federation, Princeton, 1977) p. 511.
18. S. M. BRABYN, R. COOPER and C. T. PETERS, in Proceedings of 10th International Plansee Seminar, Reutte, Metallwerk Plansee, Austria, Vol. 2, edited by H. M. Ortner (Metallwerk Plansee, Austria, 1981) p. 675.

Received 13 December 1990
and accepted 13 May 1991